

Electron Currents from Gradual Heating in Tilted Dirac Cone Materials

A. Moradpouri¹, M. Torabian¹, S. A. Jafari¹

¹ Department of Physics, Sharif University of Technology, Tehran 11155-9161, Iran
* jafari@sharif.edu

May 18, 2022

Abstract

Materials hosting tilted Dirac/Weyl fermions upgrade the solid-state phenomena into a new spacetime structure. They admit a geometric description in terms of an effective spacetime metric. Using this metric that is rooted in the long-distance behavior of the underlying lattice, we formulate the hydrodynamics theory for tilted Dirac/Weyl materials in $2 + 1$ spacetime dimensions. We find that the mingling of space and time through the off-diagonal components of the metric gives rise to: (i) heat and electric currents proportional to the *temporal* gradient of temperature, $\partial_t T$ and (ii) a non-zero Hall conductance $\sigma^{ij} \propto \zeta^i \zeta^j$ where ζ^j parametrizes the tilt in j 'th space direction. The finding (i) above that can be demonstrated in the laboratory, suggests that thanks to the non-trivial spacetime geometry in these materials, naturally available sources of $\partial_t T$ in hot deserts offer a new concept for the conversion of sunlight heating into electric energy. We further find a tilt-induced non-Drude contribution to conductivity which can be experimentally disentangled from the usual Drude pole.

Contents

1	Introduction	2
2	Hydrodynamics of tilted Dirac fermions	4
3	Emergent vector transport coefficients in tilted Dirac system:	5
3.1	Perfect fluid: Non-Drude features	7
3.2	Tilt-induced Hall response	9
3.3	Accumulative heat current	9
3.4	Vector transport coefficients	11
4	Viscous flow of tilted Dirac fermions	12
5	Summary and outlook	16
	References	18

1 Introduction

The motion of electrons in conductors in the absence of external temperature and/or electro-chemical gradients is purely random thermal motion [1]. Once a spatial temperature gradient ∇T is introduced, the vector character of ∇ specifies a preferred direction in the space, and therefore electrons flow along ∇T [2]. The purpose of this paper is to propose a class of materials where a temporal gradient $\partial_t T$ *alone* (i.e. without requiring any spatial gradient) is sufficient to generate electric and/or heat currents.

To set the stage, suppose that there is a preferred direction in the space determined by a vector ζ . In this paper we show that the anisotropy arising from such a preferred direction organizes the random motion of electrons into non-zero electric or heat currents. There are materials where such a vector ζ exists and besides, it enters the effective description of the motion of electrons in such a way that it mingles space and time coordinates and thus creates a new spacetime structure. Therefore, as we will demonstrate, a pure temporal gradient of a spatially uniform temperature T drives a current through the mixing of the space and time arising from ζ .

How do the new spacetime structures arise in the solid state? The electrons in the solids are mounted on a lattice and every periodic lattice structure belongs to one of the 230 possible space groups [3]. Some of these structures provide a low-energy effective theory for the electrons that is mathematically equivalent to the Dirac theory (e.g. in graphene [4]) or deformations of the Dirac theory as in certain structure of borophene [5, 6] or the organic compound α -(BEDT-TTF)₂I₃ [7–12] or certain deformations of graphene [13]. For the Dirac electrons in solids, the dispersion relation giving energy ε of the quasiparticles at every momentum \mathbf{k} will be a *Dirac* cone, and enjoys an *emergent Lorentz invariance* at low energies, i.e. length scales much larger than the lattice spacing [4]. But in materials hosting a tilted Dirac cone, the cone-shaped dispersion relation is tilted in energy-momentum space [13, 14]. This tilt is characterized by set of parameters ζ . Presence of the tilt in the Dirac cone, not only bestows the space with a preferred direction set by the vector ζ [13, 14], but also gives rise to an emergent spacetime structure [15–17]. In fact, it turns out that, the tilt can be attributed to an underlying metric of the spacetime [15, 18, 19]. Therefore – in the same way that Dirac materials enjoy an emergent Lorentz symmetry arising from an emergent Minkowski spacetime at long wave length for the lattice at hand – those materials that host a tilted Dirac cone can be assigned an emergent spacetime structure at long length scales. The structure of such spacetime is controlled by ζ and is given by

$$ds^2 = -v_F^2 dt^2 + (d\mathbf{r} - \zeta v_F dt)^2, \quad (1)$$

where v_F is the velocity scale that defines the emergent spacetime (which plays a role similar to the light speed c , but in real materials is two or three orders of magnitude smaller than c) and ζ encodes the tilt of the Dirac cone [19]. As such, ζ plays a role significantly more than a simple anisotropy of the space alone and specifies a metric for the effective spacetime at long wave lengths. In fact this metric is associated with the long-distance structure of the underlying (in the case of borophene, the 8pmmn) lattice and does not depend on whether the particles (excitations) are being studied are fermionic or bosonic [20, 21]. Furthermore, strong electron-electron interactions that might lead to a hydrodynamic regime studied in this paper are not able to destroy the emergent metric, as long as the symmetry of the lattice at atomic scales is intact. Only way to remove the emergent metric at long-distances is to melt the lattice. For the rest of the paper we will set $v_F = 1$. The isometries of the spacetime (1) are appropriate deformations of the Lorentz group [15]. As such, the spacetime defined by Eq. (1) is a deformation of the Minkowski spacetime by a continuous parameter ζ . The presence of tilt ζ modifies many of the physical properties of the materials, in particular including their interfaces with superconductors [22, 23]. The above metric possesses a blackhole horizon [24]

that stems from spatial variation of the Gallilean boost ζ in Eq. (1). Spatial variation of a parameter similar to ζ can emulate a black-hole horizon in atomic Bose-Einstein condensates [25], as well as in the polariton superfluids [26, 27]. The spin-polarized currents are also predicted to implement black-hole horizon for magnons [28]. Our proposal differs from the above systems and even from the tilted Dirac cone of Majorana fermions [29] in that (i) the tilted Dirac/Weyl systems required for our purpose are at ambient conditions and (ii) the quasiparticles of the theory are fermions, namely electrons and holes which carry electric charges. As such, any effects arising from the emergent structure of the spacetime, will leave direct signature in almost any electron spectroscopy experiment, including of course the transport (conductivity) measurements.

In this paper, we set out to use the hydrodynamics as a technical tool to study the electron fluid [30] in the tilted Dirac cone materials where the spacetime is given by metric (1). Let us announce our result in advance: In any conductor, the spatial gradient of temperature can generate heat and electric currents. The mingling of the spacetime in Eq. (1) will allow the materials with tilted Dirac cone to generate heat and electric currents from *pure temporal* gradients. Our theoretical tool to bring out this result is the hydrodynamics. Hydrodynamic is an effective long-time and long-distance description of quantum many body systems that focuses on few conserved collective variables rather than embarking on the formidable task of addressing all the microscopic degrees of freedom. One might wonder that at low-enough dopings where the Coulomb interactions are dominant, the structure of the spacetime given by Eq. (1) might breakdown. The direct observation of the Dirac cones in graphene – where the Coulomb interactions are strong enough to lead to hydrodynamic flow – is understood in terms of the renormalization of the Coulomb interactions. The key element is the lack of back-scattering for Dirac fermions that generates a “free Dirac fixed point” where the structure of spacetime is still Minkowski. The same conditions hold for tilted Dirac systems, and therefore one expects that the structure of the spacetime given by (1) to hold even in the hydrodynamic regime where the interactions provide the dominant scattering rates.

Hydrodynamics as a powerful universal approach, has many applications in various systems differing in microscopic details which are however, described by the same equations. Only gross symmetry properties has to be properly incorporated into the formulation of hydrodynamic for a system at hand. Applications of hydrodynamics approach in high energy physics includes quark-gluon plasma [31, 32], parity violation [33], chiral anomaly [34] and dissipative superfluid [35]. Within the hydrodynamic approach, one can come up with universal and model-independent predication such as kinematic viscosity value [36, 37]. The hydrodynamics approach can also be applied to fluid-gravity correspondence [38] which relate the dynamics of the gravity side to the hydrodynamic equations where the hydrodynamic fluctuation mode describes the fluctuations of black holes [39, 40]. In this work, we will be interested in much simpler version of hydrodynamics in a spacetime structure in $2 + 1$ dimensions subject to the metric (1) that describes electrons in sub-eV energy scales in solids with tilted Dirac cone.

The roadmap of the paper is as follows: In section 2 following Lucas [41] we formulate the hydrodynamics for the metric (1) as a natural, but categorically different generalization of the hydrodynamics theory of graphene. In section 3, in addition to the usual *tensor* transport coefficients of standards solids, we introduce *vector* transport coefficients required for a consistence treatment of the hydrodynamics in spacetime (1) where we discuss perfect fluid. It is followed by a treatment of the viscous fluids in section 4 in this new spacetime. We end the paper with discussion and summary of the paper in section 5.

2 Hydrodynamics of tilted Dirac fermions

In this section we develop the hydrodynamics of electrons in a tilted Dirac cone material. For a planar material in $d = 2$ space dimensions, there is a two-parameter family of tilt deformations given by $\vec{\zeta} = (\zeta_x, \zeta_y)$ to the Dirac equation in three dimensional spacetime. These deformations and the corresponding dispersion relation can be obtained if instead of the conventional Lorentz metric $\eta_{\mu\nu}$ one applies the following metric tensor

$$g_{\mu\nu} = \begin{pmatrix} -1 + \zeta^2 & -\zeta_j \\ -\zeta_i & \delta_{ij} \end{pmatrix}, \quad (2)$$

where $\zeta^2 = \zeta_x^2 + \zeta_y^2$ and δ is the 2×2 unit matrix [15, 19]. In this parametrization of the tilt we adopt the normalization $|\zeta| < 1$ so that spacetime makes sense in admissible coordinates. For the sake of convenience in the following computations, we introduce $\gamma = (1 - \zeta^2)^{-1/2}$. The Greek indices run over 0,1 and 2 for spacetime coordinates and the Latin indices run over spatial coordinates.

We assume that the electron-electron scattering rate τ_{ee}^{-1} take over any other scattering rate such as electron-phonon (τ_{e-ph}^{-1}) or electron-impurity scattering rate (τ_{e-imp}^{-1}). This regime is attainable in graphene that hosts upright Dirac cone [42–45]. This has become possible by ability to tune the strength of electron-electron interaction via gating that sets the scale of the Fermi surface. In such a regime, an effective description at large distances ($\gg v_F \tau_{ee}$) over long time ($\gg \tau_{ee}$) is provided by the hydrodynamics equations given by conservation laws of Noether currents. Assuming translational invariance and gauge invariance of the underlying microscopic theory, there are conserved energy-momentum tensor $T^{\mu\nu}$ and an Abelian current vector J^μ . They constitute ten independent components subject to four constraints $\partial_\mu T^{\mu\nu} = 0$ and $\partial_\mu J^\mu = 0$. We further assume that the spacetime has no torsion.

In order to find unique solutions to hydrodynamics equation, it is assumed that the currents are determined through four auxiliary local thermodynamical quantities: the temperature $T(x)$, the chemical potential $\mu(x)$, a normalized time-like velocity vector field $u^\mu(x)$ (*i.e.* $u^\mu u_\mu = -1$) and their derivatives. The *fluid observer* moves along with the fluid and measures variables (local temperature, local mass density etc.) without ambiguities. The 3-velocity u^μ is defined relative to the Eulerian (arbitrary) observer. The fluid velocity v^i is defined through $v^\mu = u^\mu / u^0$. The generalized Lorentz factor is defined as $\Gamma \equiv -n_\mu u^\mu = u^0$ where $n_\mu = (-1, \vec{0})$ is the time-like normal vector to the 2-space. An Eulerian observer attributes this factor to matter moving in the fluid frame. For instance, given the temperature measured by the fluid observer T , an Eulerian observer finds $T_E = \Gamma T$

Given an arbitrary vector, any tensor can be decomposed to its transverse and longitudinal components with respect to that vector. We have a freedom to identify u^μ with the velocity of energy flow in the so-called Landau frame $u^\mu \sim T^{\mu\nu} u^\nu$. Moreover, T and μ can be defined so that

$$u_\mu J^\mu = -n \quad \text{and} \quad u_\mu T^{\mu\nu} = -\epsilon u_\nu, \quad (3)$$

where n is the number density of charge carriers and ϵ is the energy density. In this frame, the particle current and the energy-momentum tensor can be decomposed respectively as follows [46, 47]

$$J^\mu = n u^\mu + j^\mu, \quad (4)$$

$$T^{\mu\nu} = \epsilon u^\mu u^\nu + P \mathcal{P}^{\mu\nu} + t^{\mu\nu}, \quad (5)$$

where P is a scalar, j^μ , $\mathcal{P}^{\mu\nu}$ and $t^{\mu\nu}$ are transverse tensors that satisfy $u_\mu j^\mu = u_\mu \mathcal{P}^{\mu\nu} = u_\mu t^{\mu\nu}$. Tensor t is symmetric traceless $t^\mu_\mu = 0$. Tensor \mathcal{P} is defined as

$$\mathcal{P}^{\mu\nu} = g^{\mu\nu} + u^\mu u^\nu, \quad (6)$$

which is called the projection tensor; it is symmetric and in general has non-vanishing trace. The inverse metric is

$$g^{\mu\nu} = \begin{pmatrix} -1 & -\zeta_i \\ -\zeta_j & \delta_{ij} - \zeta_i \zeta_j \end{pmatrix}. \quad (7)$$

The remaining elements P , j^μ and $t^{\mu\nu}$ are determined in terms of derivatives of hydrodynamic variables and yield the constituent equations at desired order in derivatives. At first order hydrodynamics we find

$$\begin{aligned} P &= p - \zeta_B \partial_\mu u^\mu, \\ j^\mu &= -\sigma_Q T \mathcal{P}^{\mu\nu} \partial_\nu (\mu/T) + \sigma_Q \mathcal{P}^{\mu\nu} F_{\nu\rho} u^\rho, \\ t^{\mu\nu} &= \eta \mathcal{P}^{\mu\rho} \mathcal{P}^{\nu\sigma} ((\partial_\rho u_\sigma + \partial_\sigma u_\rho - g_{\rho\sigma} \partial_\alpha u^\alpha) + \xi_B g_{\rho\sigma} \partial_\alpha u^\alpha), \end{aligned} \quad (8)$$

where p is pressure in the local rest frame, ξ_B is the bulk viscosity, σ_Q is the intrinsic conductivity and η is the shear viscosity. In the above equations, $F_{\nu\rho}$ is a tensor in 2+1 dimensions induced by an external electromagnetic field in the bulk. In passing, we recall that coefficients in zero-order hydrodynamics ϵ , p and n are fixed by T , μ and the equation of state in equilibrium thermodynamics [48–50]. Moreover, the non-negative parameters ζ_B , σ_Q and η (the Wilsonian coefficients of the effective hydrodynamic theory) are either measured in experiments or determined from an underlying microscopic (quantum) theory.

3 Emergent vector transport coefficients in tilted Dirac system:

We define the response of the electric current \vec{J} and the heat current \vec{Q} to an external electric field \vec{E} , spatial gradient $\vec{\nabla}T$ and possibly temporal variation $\partial_0 T$ of temperature as follows

$$J^i(t) = \int dt' \left[\sigma^{ij} E_j(t') - \alpha^{ij} \partial_j T(t') - \beta^i T(t') \partial_0 \frac{\mu(t')}{T(t')} \right], \quad (9)$$

$$Q^i(t) = \int dt' \left[T \bar{\alpha}^{ij} E_j(t') - \bar{\kappa}^{ij} \partial^j T(t') - \mu \gamma^i T(t') \partial_0 \frac{\mu(t')}{T(t')} \right], \quad (10)$$

where σ^{ij} , α^{ij} , $\bar{\alpha}^{ij}$ and $\bar{\kappa}^{ij}$ are the usual tensor response coefficients relating the electric and heat currents to spatial gradients of electrochemical potential or temperature [2]. Anticipating electric/heat currents in response to temporal gradient $\partial_0 T$, we have additionally introduced the *vector transport coefficients* β^i and γ^i . All the above coefficients are functions of $t - t'$ by time-translational invariance.

We compute the above transport coefficients within hydrodynamics theory. We imagine that fluid is perturbed around its equilibrium state (specified by μ_0 , T_0 and $u_0^\mu = (1 - \zeta^2)^{-1/2} (1, \vec{0})$ in the rest frame of the fluid exposed to $\vec{E}_0 = \vec{0}$) by a slight amount parametrized as follows

$$\delta T(t, \vec{x}), \quad \delta u^\mu(t, \vec{x}) = \gamma (\gamma^2 \vec{\zeta} \cdot \delta \vec{v}, \delta \vec{v}), \quad \delta \vec{E}(t, \vec{x}). \quad (11)$$

The linear response of the electric current is given by

$$\delta J^i = n \gamma \delta v^i - \sigma_Q \zeta^i \frac{\mu_0}{T_0} \partial_0 \delta T - \sigma_Q g^{ij} \left(\gamma \delta E_j - \frac{\mu_0}{T_0} \partial_j \delta T \right). \quad (12)$$

Moreover, the leading order perturbation in derivatives is

$$\begin{aligned} \delta T^{0i} &= \gamma^2 (\epsilon_0 + p_0) \delta v^i - \delta P \zeta^i \\ &+ \eta \gamma^2 \zeta^2 \zeta^i (2 \partial_0 \delta u_0 - g_{00} \partial_\alpha \delta u^\alpha) \end{aligned} \quad (13)$$

$$\begin{aligned}
& - \eta(\zeta^j \zeta^i + \gamma^2 \zeta^2 g^{ij})(\partial_0 \delta u_j + \partial_j \delta u_0 - g_{0j} \partial_\alpha \delta u^\alpha) \\
& + \eta \zeta^j g^{ik} (\partial_j \delta u_k + \partial_k \delta u_j - g_{jk} \partial_\alpha \delta u^\alpha) + \xi \zeta^i \partial_\alpha \delta u^\alpha.
\end{aligned}$$

Here δP and δv^i are changes in pressure and velocity caused by the probe (external) electric field or temperature gradients and are first order in the probe fields. Using the above equation we can compute thermal conductivity through

$$\delta Q^i = \delta T^{0i} - \delta(\mu J^i). \quad (14)$$

An interesting feature of Eq. (8) in the tilted Dirac/Weyl materials is a genuine effect where temporal variations generate currents: We note that in a linear hydrodynamic theory the term in the brackets in this equation are already first order, and therefore at this order $\mathcal{P}^{\mu\nu} \rightarrow g^{\mu\nu}$. Therefore the spatial component J^i of the current (in addition to the first term nu^i) will acquire a contribution proportional to $\partial_0 \mu$ and $\partial_0 T$ which is accompanied by the tilt parameters $g^{i0} = -\zeta^i$. This effect is solely dependent on the tilt parameters ζ^i and vanishes for upright Dirac/Weyl systems where $\zeta^i = 0$. Therefore, we extend the conventional thermoelectric coefficients to account for this through additional transport coefficients β^i and γ^i in Eqns. (9) and (10).

We solve the hydrodynamics equations to evaluate the electric current and thermal current in the presence of background electric field and temperature spatiotemporal gradients. At this leading order, the charge conservation $\partial_\mu J^\mu = 0$ implies

$$\partial_t \left[\gamma \delta n - n \gamma^3 \zeta_i \delta v^i + \frac{\mu_0}{T_0} \sigma_Q (\gamma^2 \zeta^2 \partial_0 - \zeta^i \partial_i) \delta T + \sigma_Q \zeta^i \gamma \delta E_i \right] + \partial_i (\delta J^i) = 0. \quad (15)$$

Similarly, the energy conservation $\partial_\mu T^{\mu 0} = 0$ implies

$$\begin{aligned}
& \partial_t \left[\gamma^2 \delta \epsilon + \gamma^2 \zeta^2 \delta p - 2\gamma^4 (\epsilon_0 + p_0) \zeta_i \delta v^i - \eta \gamma^4 \zeta^4 (2\partial_0 \delta u_0 - g_{00} \partial_\alpha \delta u^\alpha) \right. \\
& \quad \left. + 2\eta \zeta^2 \gamma^2 \zeta^i (\partial_i \delta u_0 + \partial_0 \delta u_i - g_{i0} \partial_\alpha \delta u^\alpha) - \eta \zeta^i \zeta^j (\partial_i \delta u_j + \partial_j \delta u_i - g_{ij} \partial_\alpha \delta u^\alpha) - \xi \gamma^2 \zeta^2 \partial_\alpha u^\alpha \right] \\
& + \partial_i \delta T^{i0} = 0.
\end{aligned} \quad (16)$$

Finally, the momentum conservation $\partial_\mu T^{\mu i} = 0$ gives

$$\begin{aligned}
-\frac{\epsilon_0 + p_0}{\tau_{\text{imp}}} \delta u^i & = \partial_0 (\delta T^{0i}) + \partial_i \left[\delta P g^{ij} - \eta \zeta^i \zeta^j (2\partial_0 \delta u_0 - g_{00} \partial_\alpha \delta u^\alpha) \right. \\
& \quad \left. + \eta (\zeta^i g^{jk} + \zeta^j g^{ik}) (\partial_0 \delta u_k + \partial_k \delta u_0 - g_{0k} \partial_\alpha \delta u^\alpha) \right. \\
& \quad \left. - \eta g^{il} g^{kj} (\partial_l \delta u_k + \partial_k \delta u_l - g_{lk} \partial_\alpha \delta u^\alpha) - \xi g^{ij} \partial_\alpha \delta v^\alpha \right],
\end{aligned} \quad (17)$$

where the parameter τ_{imp} is the relaxation time due to scattering from impurities. The above expressions in the square bracket are leading order perturbations in number density, energy, density and the stress tensor. We apply equations (15), (16) and (17) to extract transport coefficients. In passing we note that, in the fluid rest frame the electric field, the temperature gradient and the pressure gradient are balanced as $-\partial_i P = nE_i + s\partial_i T$. Thus, we apply the following constraint

$$-\partial_i \delta P = n_0 \delta E_i + s_0 \partial_i \delta T, \quad (18)$$

in the leading order in perturbations.

3.1 Perfect fluid: Non-Drude features

We start by ignoring dissipation $\eta = \xi = 0$, Furthermore, we are interested in a homogeneous flow; *i.e.* spatially uniform solutions with $\partial_j \delta v^i = 0$. With these assumptions, the energy-momentum conservation implies

$$\partial_t \left[\gamma^2 (\delta \epsilon + \zeta^2 \delta P) - 2\gamma^4 (\epsilon_0 + p_0) \zeta_j \delta v^j \right] - \zeta^i \partial_i \delta P = 0, \quad (19)$$

$$\partial_t \left[\gamma^2 (\epsilon_0 + p_0) \delta v^i - \zeta^i \delta P \right] + g^{ij} \partial_j \delta P = -\frac{\epsilon_0 + p_0}{\tau_{\text{imp}}} \gamma \delta v^i. \quad (20)$$

After a Fourier transformation in time, the above equations can be solved for the velocity perturbation as

$$\delta v^i = (\mathcal{C}^{-1})_j^i \left[g^{kj} - \frac{\zeta^j \zeta^k}{\gamma^2 (2 + \zeta^2)} \right] (-\partial_k \delta P), \quad (21)$$

where \mathcal{C}^{-1} is the inverse matrix of

$$\mathcal{C}_j^i = \left[\gamma \frac{\epsilon_0 + p_0}{\tau_{\text{imp}}} (1 - i\gamma\omega\tau_{\text{imp}}) \right] \delta_j^i + \left[2i\omega\gamma^2 \frac{\epsilon_0 + p_0}{2 + \zeta^2} \right] \zeta^i \zeta_j, \quad (22)$$

which is explicitly computed in the appendix. Then, we compute the electric current (12) as a response to spatiotemporal variation of the electric field and temperature. Finally, by applying equations (18) and (21) we can read the coefficients in (9) as follows

$$\sigma^{ij} = \gamma n_0^2 (\mathcal{C}^{-1})_k^i \left[g^{kj} - \frac{\zeta^j \zeta^k}{\gamma^2 (2 + \zeta^2)} \right] - g^{ij} \gamma \sigma_Q, \quad (23)$$

$$\alpha^{ij} = -\gamma n_0 s (\mathcal{C}^{-1})_k^i \left[g^{kj} - \frac{\zeta^j \zeta^k}{\gamma^2 (2 + \zeta^2)} \right] - \frac{\mu_0}{T_0} \sigma_Q g^{ij}, \quad (24)$$

$$\beta^i = -\sigma_Q \zeta^i. \quad (25)$$

The pole structure of the electric and heat conductivity tensors are the same. This is because they are both related to the determinant of the matrix \mathcal{C} . Therefore, we focus on the poles of the conductivity. We find that the conductivity tensor has the following two poles

$$\omega_1 = \frac{-i}{\gamma\tau_{\text{imp}}} \equiv \frac{-i}{\tau_{\text{imp}}^{\text{lab}}}, \quad (26)$$

$$\omega_2 = \frac{2 + \zeta^2}{2 - \zeta^2} \omega_1. \quad (27)$$

In the upright Dirac cone with Minkowski spacetime structure, $\zeta \rightarrow 0$, both poles ω_1 and ω_2 of Eqns. (26) and (27) reduce to the Drude result. To understand these poles, we have defined a *red-shifted relaxation time* $\tau_{\text{imp}}^{\text{lab}} = \gamma\tau_{\text{imp}}$. In this definition τ_{imp} can be interpreted as the microscopic relaxation time experienced by electrons in the spacetime with a given ζ , while $\tau_{\text{imp}}^{\text{lab}}$ can be interpreted as the same time measured in the laboratory by the experimentalist sitting in the laboratory spacetime having $\zeta = 0$. As such, the pole at ω_1 is a natural extension of the Drude pole to the geometry (1). However, the new pole ω_2 arises from the new spacetime structure. Although at $\zeta \rightarrow 0$ limit it becomes degenerate with the Drude pole, but at $\zeta \rightarrow 1$ it can become up to 3 times larger than ω_1 . Both poles are on the imaginary axis, and their real part is zero, as they are caused by very low-energy (Drude) excitations across the Fermi level. Then the question will be, is there a way to distinguish the

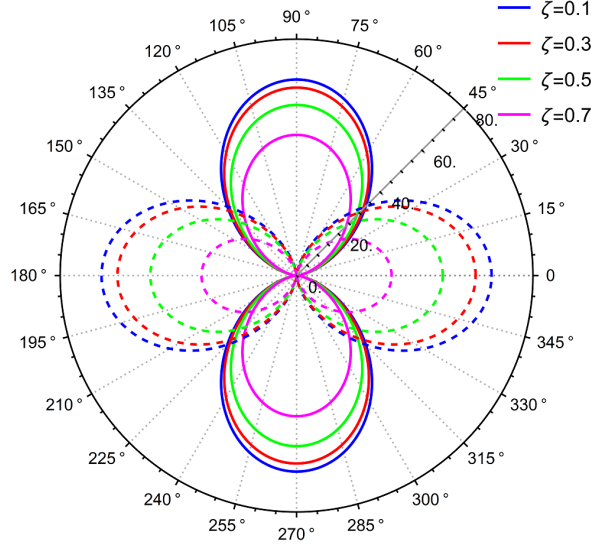


Figure 1: Polar dependence of residue of the longitudinal conductivity σ^{xx} for Drude like pole ω_1 (solid lines) and spacetime pole ω_2 (dashed lines) in units of $[\frac{1}{mev \cdot \tau_{imp}^2}]$. The polar angle is measured from the direction of the tilt vector ζ .

contributions from the Drude pole ω_1 and the spacetime pole ω_2 ? To answer this question, we need to look at the residues at the two poles that determine the spectral intensity associated with each pole.

Let us start by looking at the residue of the absorptive part of the conductivity, namely the longitudinal conductivity σ^{xx} . The residues at the above poles are computed as follows¹

$$\text{Res}(\sigma_{\omega_1}^{xx}) = \frac{n^2 v^2 \zeta_y^2}{\epsilon_0 + p_0 \gamma \zeta^2}, \quad (28)$$

$$\text{Res}(\sigma_{\omega_2}^{xx}) = \frac{2n^2 v^2 \zeta_x^2}{\epsilon_0 + p_0 \gamma^3 (2 - \zeta^2) \zeta^2}. \quad (29)$$

By symmetries of space time σ^{yy} can be extracted from σ^{xx} only by exchanging $\zeta_x \leftrightarrow \zeta_y$. So there is no new information in residues of the poles of σ^{yy} .

As pointed out, both ω_1 and ω_2 poles are on the imaginary axis and their real part is zero. To disentangle their contribution, note that the meaning of the longitudinal conductivity σ^{xx} is the current along the applied electric field (both assumed along the x direction). But then the x axis can subtend an angle θ with the tilt vector ζ . This can be an interesting variable. Therefore, in Fig. 1 we have plotted the dependence of the residues of the longitudinal part of the conductivity on the polar angle θ of the tilt vector. The solid (dashed) lines correspond to the Drude-like pole ω_1 (spacetime pole ω_2). Various colors correspond to different tilt magnitudes. Both poles have a dipolar pattern. But their nodal structure is different which helps to identify which pole is contributing the spectral weight. When the electric field is applied along the tilt direction ($\theta = 0$), the residue of the Drude-like pole vanishes and the absorption is contributed by ω_2 pole. By rotating the applied electric field away from

¹In all plots of this paper, the Fermi velocity v_F has been explicitly included and expressed in units of $[\frac{r}{\tau_{imp}}]$ where r is a length scale corresponding to average one electron and is related to the density by $nr^2 = 1$. For typical $n \sim 10^{12} \text{cm}^{-2}$, we get $r = 10^{-6} \text{cm}$. Furthermore a typical value of τ_{imp} is equal to 10^{-13}s .

the tilt direction, the Drude-like pole ω_1 takes over the spacetime pole ω_2 . When the applied electric field is completely perpendicular to ζ , only ω_1 contributes to the conductivity. The common feature of solid and dashed curves in Fig. 1 is that the spectral weight of both ω_1 and ω_2 poles decreases by increasing the tilt ζ .

3.2 Tilt-induced Hall response

Another unusual effect arising from the tilt in ideal fluid is the presence of a non-zero Hall and thermal Hall coefficients *in the absence of external magnetic field*. Due to off-diagonal metric elements of the metric $g^{ij} \propto \zeta^i \zeta^j$, a non-zero Hall and thermal Hall coefficient proportional to $\zeta^i \zeta^j$ appear in Eqs. (23) and (24). This effect also solely depends on the presence of the tilt ζ^i . Mathematically, in the absence of ζ^i (isotropic space), the conductivity tensor σ^{ij} (as in the case of graphene) will become proportional to δ^{ij} . But in the present case, the anisotropy of the space will be reflected in a $\zeta^i \zeta^j$ dependence in all tensorial quantities including the conductivity and heat conductivity tensors. As such, the non-zero Hall and thermal Hall coefficients in the tilted Dirac cone can be directly attributed to the structure of the spacetime.

Now let us consider the off-diagonal (transverse) component of the conductivity, namely σ^{xy} . It turns out that there will be a tilt-induced Hall response σ^{xy} which is given by

$$\text{Res}(\sigma_{\omega_1}^{xy}) = -\frac{n^2 v^2}{\epsilon_0 + p_0} \frac{\zeta_x \zeta_y}{\gamma \zeta^2}, \quad (30)$$

$$\text{Res}(\sigma_{\omega_2}^{xy}) = \frac{2n^2 v^2}{\epsilon_0 + p_0} \frac{\zeta_x \zeta_y}{\gamma^3 (2 - \zeta^2) \zeta^2}. \quad (31)$$

Mathematically, σ^{ij} (and also α^{ij}) being tensors are naturally expected to have a term proportional to $g^{ij} \sim \zeta^i \zeta^j$. But what is the physical meaning of a non-zero Hall coefficient in the absence of a background B_z in the new spacetime geometry? Indeed in the small tilt limit, the metric (1) can be viewed as a superposition of an additional "Lorentz" boost with the boost parameter given by ζ [51]. As such the applied electric field can act like an effective B-field, generating the Hall response. But note that our finding is not limited to small ζ and is valid for any finite ζ . The residues of the Hall conductivity arising from ω_1 and ω_2 poles are plotted in Fig. 2. As can be seen both poles display quadrupolar pattern. Also their behavior with ζ is similar. Both intensities decrease upon decreasing the tilt magnitude ζ .

The conclusion is that, the longitudinal conductivity is a suitable measure to disentangle the role of Drude-like pole ω_1 and spacetime pole ω_2 in the conductivity of tilted Dirac material sheets.

3.3 Accumulative heat current

Now let us turn our attention to the heat (energy) transport coefficients. The thermal current in a non-viscous homogeneous fluid is given by

$$Q_i = \gamma^2 (\epsilon_0 + p_0) \delta v_i - \zeta_i \delta P - \mu_0 \delta J_i, \quad (32)$$

where δJ_i is given in (12). We use the energy conservation equation (19) and equation of state $\epsilon = 2 \cdot P$ to compute the pressure perturbation δP as follows

$$\delta P(t) = \frac{\gamma^2}{2 + \zeta^2} \left[2(\epsilon_0 + p_0) \zeta_j \delta v_j + \gamma^{-2} \zeta_j \int^t dt' \partial_j \delta P(t') \right]. \quad (33)$$

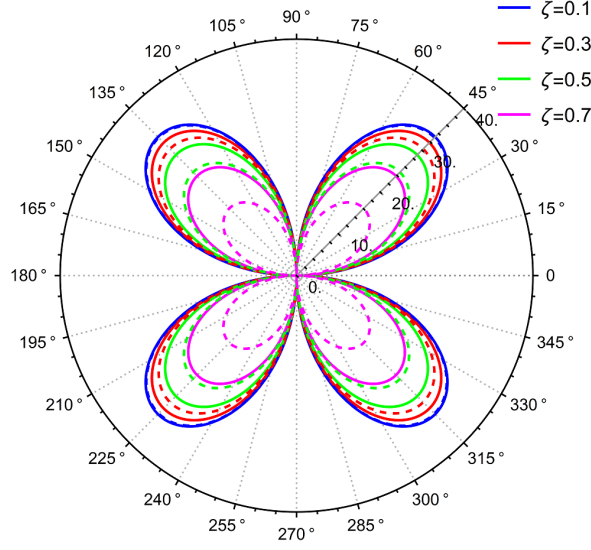


Figure 2: Polar dependence of residue of σ^{xy} for ω_1 (solid lines) and ω_2 (dashed lines) in units of $[\frac{1}{mev.\tau_{imp}^2}]$. The polar angle denotes the angle between the applied electric field and the tilt vector ζ .

Ignoring the last term in the above equation, we compute the coefficients in thermal current (10) by applying equation (18), (21), (32) and (33) as follows

$$\bar{\alpha}^{ij} = \frac{n_0}{T_0} \mathcal{I}_m^i (C^{-1})_k^m \left[g^{kj} - \frac{\zeta^j \zeta^k}{\gamma^2 (2 + \zeta^2)} \right] + \gamma \frac{\mu_0}{T_0} \sigma_Q g^{ij}, \quad (34)$$

$$\bar{\kappa}^{ij} = s \mathcal{I}_m^i (C^{-1})_k^m \left[g^{kj} - \frac{\zeta^j \zeta^k}{\gamma^2 (2 + \zeta^2)} \right] - \frac{\mu_0^2}{T_0} \sigma_Q g^{ij}, \quad (35)$$

$$\gamma^i = -\sigma_Q \zeta^i, \quad (36)$$

where \mathcal{I}_j^i is defined as

$$\mathcal{I}_j^i = \left[\gamma^2 (\epsilon_0 + p_0) - \gamma \mu_0 n_0 \right] \delta_j^i - \left[2\gamma^2 \frac{\epsilon_0 + p_0}{2 + \zeta^2} \right] \zeta^i \zeta_j. \quad (37)$$

The last term in (33) gives an additional contribution to $\bar{\alpha}^{ij}$ and $\bar{\kappa}^{ij}$. To see how the effect of the last term can be measured, let us consider the dc limit $\omega = 0$. In this limit the above equations are regular and well behaved. This last term in the absence of dependence on the time argument t' will give a term in the heat current which has the following form ²,

$$Q^i(t) \supset t \frac{\gamma^{-2}}{2 + \zeta^2} \zeta^i \zeta^j (n \delta E_j + s \partial_j \delta T). \quad (38)$$

The above equation has directly measurable consequence: Irrespective of whether the tilted Dirac cone system is stimulated by external electric field or external temperature gradient, an *accumulative* heat current will be generated in the system which is proportional to the time t during which the external

²Note that the notation \supset means that the left hand side contains a term of the form given in the right hand side.

field is applied. This heat current is (i) in the direction of $\vec{\zeta}^3$ and (ii) is controlled by the component of $\delta\vec{E}$ (or $\vec{\nabla}\delta T$) along the $\vec{\zeta}$. The resulting dipolar angular profile can be used to immediately map the direction of the vector $\vec{\zeta}$. Put it another way, the latter means that the accumulative heat current vanishes if the externally applied field or temperature gradient is transverse to the tilt vector $\vec{\zeta}$. The accumulative nature (proportionality to time t during which the external field is applied) of this heat current means that if the experiment is performed for a long enough time t , it can take over any other terms in the heat current given in Eqns. (34, 35). This increase can not be continued indefinitely, as beyond certain point, nonlinear effects take over, and the linear response ceased to be valid.

This effect solely depends on the presence of a tilt vector $\vec{\zeta}$, and as such has no analog in other solid-state systems. The peculiar $\vec{\zeta}$ dependence along with a t -linear dependence of this particular form of heat current can be employed to separate it from the other terms in the heat current. The anomalous heat transport in $8Pmmn$ borophene studied in Ref. [52] can be re-examined in the light of this new term.

3.4 Vector transport coefficients

One striking aspect of the transport of heat and electric currents in tilted Dirac cone systems is the appearance of new transport coefficients, β^i and γ^i which are given by equations (25) and (36), respectively. These *vector* transport coefficients (as opposed to tensor transport coefficients) relate the temporal gradients of electrochemical potential and temperature to electric and heat currents. As can be seen from Eqns. (25) and (36), at the present order of calculations, these are frequency independent and are furthermore proportional to the only available vector, namely ζ^i . The fact that these vector transport coefficients are given by product of σ_Q and ζ^i , means that these coefficients quantifying the conversion of temporal gradients to electric and heat currents are essentially determined by the ability σ_Q of the material to conduct (electricity). In the absence of tilt in normal conductors, since the vector ζ^i is zero, there will be no preferred direction in the space, and therefore the vector transport coefficients γ^i and β^i remain inert. In tilted Dirac materials, these vector transport coefficients find a unique opportunity to become active and play a significant role. Generally, there can be materials with odd number of Dirac valleys [53]. But quite often, the Dirac cones come in pairs. This has to do with Fermion doubling problem according to which, putting a Dirac theory on a (hypercubic) lattice doubles the number of Dirac fermions [54]. In the former case where the number of Dirac nodes is odd, there is no challenge and the vector transport coefficients are already active. But the latter case corresponding to lattices on which Fermion doubling occurs, requires some discussion: If the material is inversion symmetric, its two valleys come with tilt parameters $\zeta_{\pm} = \pm\zeta$ [19]. Since the number of Dirac valleys is even, the currents from the two valleys cancel each other. Therefore, despite that the β^i and γ^i transport coefficients for a single valley are active, for the whole material hosting even number of valleys they cancel each other's effect in an *infinite* system. However, if the material lacks an inversion center such that $\zeta_+ + \zeta_-$ becomes non-zero, then a net electric (heat) current enabled by the coefficient β^i (γ^i) can flow in response to temporal gradient of temperature (or electrochemical potential if one wishes to make it depend on time). Therefore one possible route to realization of the present effect is to search for a tilted Dirac cone in a material without inversion center.

The second route can be built around the ideas of "valleytronics" [55] that are popular in planar (2D) materials. The essential idea is that imposing appropriate boundary condition by cutting appropriate edges, one can create valley valves [56] at the other end of which the "population" of the two

³In the absence of a vector $\vec{\zeta}$ in the spacetime, all directions are equivalent. For the tilted Dirac materials, besides modifying the metric of the spacetime, the vector $\vec{\zeta}$ specifies a preferred direction in the space. Therefore the proportionality of $\vec{Q} \propto \vec{\zeta}$ is intuitively appealing.

valleys is imbalanced. In this approach, although the material is inversion symmetric and has even number of valleys with opposite tilt parameters $\pm\zeta$, that cancel out for *infinite* system, in finite systems with appropriate boundaries, the population imbalance between the valleys gives rise to a net electric current $\sim \beta^i(n_+ - n_-)$ or heat current $\sim \gamma^i(n_+ - n_-)$ which is driven by the imbalanced population of the symmetric valleys.

The surface of crystalline topological insulators is also predicted to host tilted Dirac cone [57]. To exploit only one Dirac cone, one needs to employ the semi-infinite geometry which is not useful for practical uses. In practice the systems have finite thickness, and therefore the other tilted Dirac cone at the other surface will nearly cancel the effect of the first.

4 Viscous flow of tilted Dirac fermions

So far we have brought up essential physics of TDFs for ideal fluid of electrons. It is now expedient to discuss the effect of viscosity in such systems. In this case, the energy and momentum conservation equations in Fourier space are respectively given as follows

$$-i\omega\delta P = \frac{\gamma^2}{2+\zeta^2} \left[-2i\omega(\epsilon_0 + p_0) + \zeta^2\gamma\omega^2(\eta + \xi) \right] \zeta_j \delta v^j + \frac{1}{\gamma^2(2+\zeta^2)} \zeta^j \partial_j \delta P, \quad (39)$$

$$\left[g^{kj} - \frac{\zeta^j \zeta^k}{\gamma^2(2+\zeta^2)} \right] (-\partial_j \delta P) = \left[\gamma \frac{\epsilon_0 + p_0}{\tau_{\text{imp}}} (1 - i\omega\gamma\tau_{\text{imp}}) \delta_j^i + 2i\omega\gamma^2 \frac{\epsilon_0 + p_0}{2+\zeta^2} \zeta^i \zeta_j \right. \\ \left. - \eta\omega^2\gamma^3 \left(\frac{4+3\zeta^2}{2+\zeta^2} \zeta^i \zeta_j + \zeta^2 \delta_j^i \right) - \xi\omega^2\gamma^3 \frac{2}{2+\zeta^2} \zeta^i \zeta_j \right] \delta v^j. \quad (40)$$

Solving for the perturbation in the velocity field we find

$$\delta v^i = (\mathcal{F}^{-1})_k^i \left[g^{kj} - \frac{\zeta^j \zeta^k}{\gamma^2(2+\zeta^2)} \right] (-\partial_j \delta P), \quad (41)$$

where \mathcal{F}^{-1} is the inverse matrix of

$$\mathcal{F}_j^i = \mathcal{C}_j^i - \eta\omega^2\gamma^3 \left[\frac{4+3\zeta^2}{2+\zeta^2} \zeta^i \zeta_j + \zeta^2 \delta_j^i \right] - \xi\omega^2\gamma^3 \frac{2}{2+\zeta^2} \zeta^i \zeta_j, \quad (42)$$

and \mathcal{C} is the same as Eq. (22) for dissipationless fluid. The explicit form of inverse matrix is presented in the appendix. Then similar to the no-viscous fluid, by applying equations (12), (18) and (41) we can read the coefficients in (9) as

$$\sigma^{ij} = \gamma n_0^2 (\mathcal{F}^{-1})_k^i \left[g^{kj} - \frac{\zeta^j \zeta^k}{\gamma^2(2+\zeta^2)} \right] - g^{ij} \gamma \sigma_Q, \quad (43)$$

$$\alpha^{ij} = -\gamma n_0 s (\mathcal{F}^{-1})_k^i \left[g^{kj} - \frac{\zeta^j \zeta^k}{\gamma^2(2+\zeta^2)} \right] - \frac{\mu_0}{T_0} \sigma_Q g^{ij} \\ = -\frac{s}{n_0} \sigma^{ij} - g^{ij} \sigma_Q \left(\frac{\mu_0}{T_0} + \gamma \frac{s}{n_0} \right), \quad (44)$$

where just the matrix \mathcal{F} encompassing viscosity parameters replaces matrix \mathcal{C} of non-viscous case.

The bulk viscosity at this order can be ignored [41] and shear viscosity can be controlled by temperature and its dependence for graphene is as follow [42]:

$$\eta = 0.45 \frac{(k_B T)^2}{\hbar (v_F \alpha)^2}, \quad (45)$$

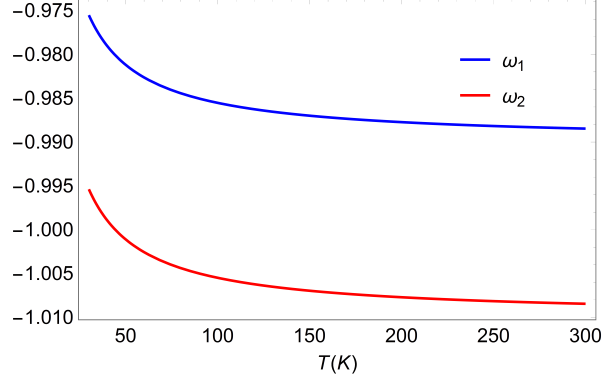


Figure 3: Temperature dependence of roots at fixed $\zeta_x = \zeta_y = 0.1$

where $\alpha = c\alpha_{\text{QED}}/(\varepsilon_r v_F)$ and ε_r is the relative permeability of the material with respect to vacuum and α_{QED} is the fine structure constant. Essential scales here are temperature and the kinetic energy of the Dirac electrons set by v_F . Since v_F in TDFs is comparable to graphene, we expect this formula to give reasonable estimate of η in TDFs.

Moreover, we find the coefficients in thermal current (10) by using equation (18), (41), (32) and (33) as

$$\bar{\alpha}^{ij} = \frac{n_0}{T_0} (\mathcal{I}_m^i + i\omega \mathcal{V}_m^i) (\mathcal{F}^{-1})_k^m \left[g^{kj} - \frac{\zeta^j \zeta^k}{\gamma^2 (2 + \zeta^2)} \right] + \gamma \frac{\mu_0}{T_0} \sigma_Q g^{ij}, \quad (46)$$

$$\begin{aligned} \bar{\kappa}^{ij} &= s (\mathcal{I}_m^i + i\omega \mathcal{V}_m^i) (\mathcal{F}^{-1})_k^m \left[g^{kj} - \frac{\zeta^j \zeta^k}{\gamma^2 (2 + \zeta^2)} \right] - \frac{\mu_0^2}{T_0} \sigma_Q g^{ij} \\ &= s \frac{T_0}{n_0} \bar{\alpha}^{ij} - g^{ij} \sigma_Q \frac{\mu_0}{T_0} (\mu_0 + \gamma s), \end{aligned} \quad (47)$$

where \mathcal{I} is defined through (37) for dissipationless fluid and \mathcal{V}_j^i encodes the viscosity information as follows:

$$\mathcal{V}_j^i = \eta \gamma^3 \zeta^2 \left(\delta_j^i - \frac{1}{2 + \zeta^2} \zeta^i \zeta_j \right) + \xi \gamma \frac{1}{2 + \zeta^2} \zeta^i \zeta_j. \quad (48)$$

As can be seen, viscosity are given by zeros of determinant of matrix \mathcal{F} which is now a fourth degree polynomial and it must have two extra poles. It turns out that only two of these poles are causal and reduce to the ω_1 and ω_2 poles of the ideal fluid in Eq. (26) and (27). As can be seen in Fig. 3 the poles do not alter much by viscosity (which is controlled by temperature). In Fig. 4 we have polar plotted the residue of the σ^{xx} at the ω_1 (solid lines) and ω_2 (dashed lines) poles. Similarly in Fig. 5 we have plotted the same information for the Hall conductance σ^{xy} . As can be seen the two figures 4 and 5 parallel their ideal counterparts in Figs. 1 and 2, respectively. As can be seen their qualitative features are identical. So we do not expect the viscosity to heavily affect the conductivity of the TDFs.

To see this in a more quantitative setting, in Fig. 6, we have polar plotted the residues of the longitudinal conductivity σ^{xx} for the viscous flow (solid line) and ideal flow (dashed lines). As before, the vertical lobe (blue) corresponds to the Drude-like pole ω_1 , while the horizontal lobe (red) corresponds to the spacetime pole ω_2 . Fig. 6 nicely shows how the viscous flow is continuously connected to the ideal flow. One further information that can be extracted from this figure is that the spectral intensity in ideal flow is larger than the viscous flow. Although the quantitative difference is small, but it shows that the light can be better absorbed by the viscous TDFs than the ideal TDFs.

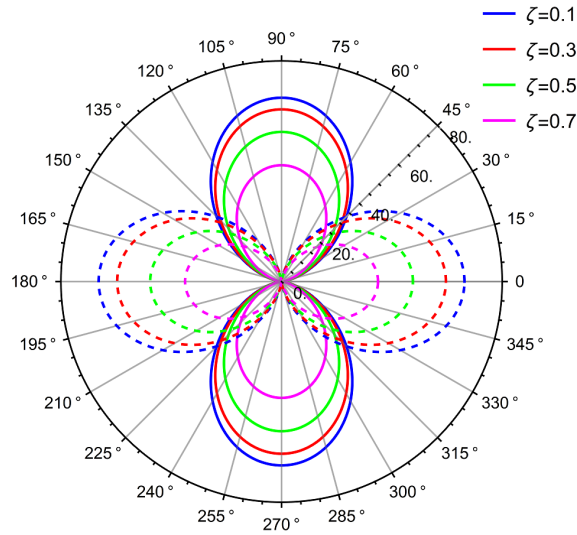


Figure 4: Polar dependence of residue of σ^{xx} for ω_1 (solid lines) and ω_2 (dashed lines) in units of $[\frac{1}{\text{mev} \cdot \tau_{\text{imp}}^2}]$ for viscous fluid at $T = 150\text{K}$.

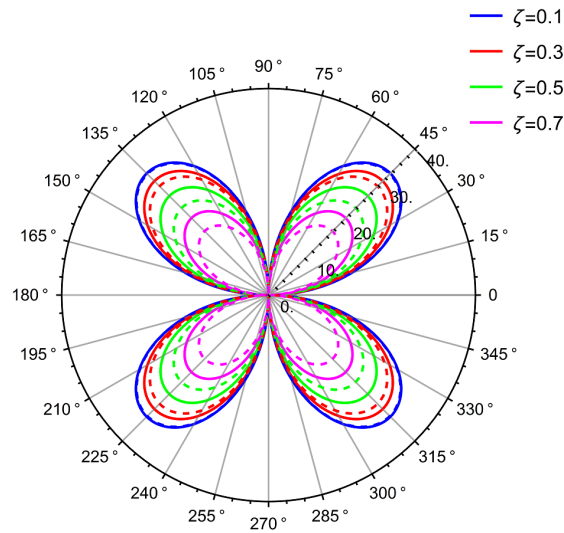


Figure 5: Residues at the poles ω_1 (solid) and ω_2 (dashed) of the σ^{xy} for viscous flow at $T = 150\text{K}$.

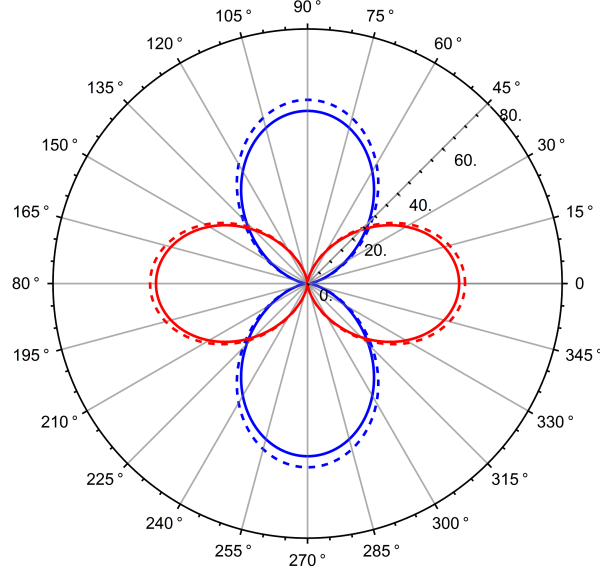


Figure 6: Comparison between the angular dependence of the residue of σ^{xx} at fixed $\zeta = 0.5$ for viscous fluid (solid-lines) and ideal fluid (dashed lines). The poles ω_1 and ω_2 are shown by blue and red color. Spectral weights are larger for ideal fluid of TDFs.

Now that we have given a comprehensive comparison between the conductivity tensor for the ideal and viscous flow of TDFs, we are ready to present the actual experimentally expected conductivity lineshapes. As noted in Eq. (26) and (27), and their viscous extensions in Fig. 3, both poles are purely imaginary and their real part is zero. This conforms to the intuition, as in a Fermi surface built on a tilted Dirac cone dispersion, one does not expect higher energy absorptions to take place. One still has the low-energy particle-hole excitations across the Fermi surface.

Fig. 7 shows the real (solid line) and imaginary (dashed line) parts of the longitudinal conductivity σ^{xx} for the fluid of TDFs. The viscosity corresponds to $T = 150\text{K}$. The angle is chosen to be $\theta = \pi/4$ because as we learned from Figs. 1 and 4, along this direction both ω_1 and ω_2 poles comparably contribute. As can be seen, larger tilt values reduce the height of the Drude peak. Figure 8 shows the same information as Fig. 7 for the Hall conductivity σ^{xy} . Again we have plotted this curve for $\theta = \pi/4$ at which both poles have comparable contributions as demonstrated in Figs. 2 and 5. The Hall conductivity in contrast to the longitudinal conductivity shows enhancement of the central peak upon increasing the tilt ζ .

Now that we are done with the viscosity dependence of the tensor conductivity σ^{ij} , let us comment about the effect of viscosity on vector transport coefficients. Since the shear viscosity η does not enter the definition of the charge current, the presence of viscosity does not change the vector transport coefficients β^i and γ^i . Note further that in the presence of viscosity, the transport coefficients α and $\bar{\alpha}$ will not be the same. The explicit form of the transport coefficients are given in the appendix.

Finally, we turn to the accumulative current in non-ideal fluid: As long as the velocity field is homogeneous, the shear viscosity η does not modify the energy equation (16). Therefore when combined with the heat current equation, it will not lead to any modification in the accumulative current. The conclusion is that, the accumulative current is not affected by viscous forces.

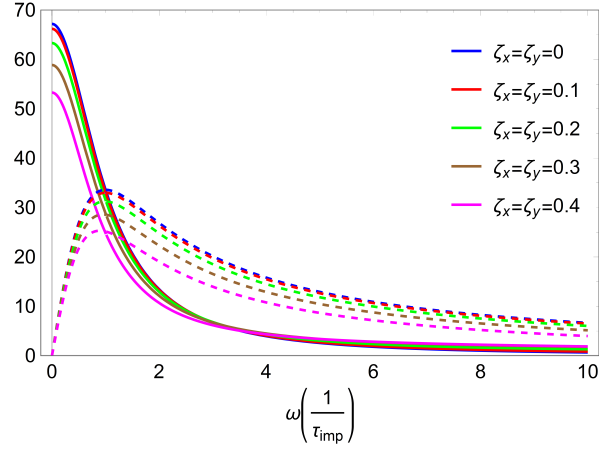


Figure 7: Real part (solid-lines) and imaginary part (dashed-lines) of σ^{xx} for viscous fluid of TDFs at $T=150$ K in units of $[\frac{1}{mev \cdot \tau_{imp}}]$. The hidden structure inside the broad Drude peak can be revealed by polar dependence in Figs. 1 and 4.

5 Summary and outlook

In this paper, we have investigated the hydrodynamics of tilted Dirac fermions that live in the tilted Dirac materials. The essential feature of these materials is that the "tilt" deformation of the Dirac (or Weyl if we are in three space dimensions) can be neatly encoded into the spacetime metric. As such, these materials are bestowed with an emergent spacetime geometry which distinguishes them from the rest of solid state systems. This metric encodes the long-distance structure of the complicated and rich content of the 8pmmn lattice. Putting it another way, the 8pmmn point group symmetry of the atomic scales becomes a metric at long wave-length scales [20, 21]. Therefore even the strong electron-electron interactions responsible for the formation of the hydrodynamic regime are not able to destroy this metric structure as long as the lattice is not molten. What our hydrodynamics theory in this paper predicts is that the mixing of space and time coordinates in such solids gives rise to transport properties which have no analogue in other solid state systems where there is no mixing between space and time coordinates.

The first non-trivial consequence of the spacetime structure determined by tilt parameters ζ^i is that it gives rise to off-diagonal (Hall) transport coefficients *in the absence of magnetic field*. These Hall coefficients appear in both charge and heat transport. By generic symmetry structure of the spacetime in such solids, the conductivity tensors will be proportional to $g^{ij} = \delta^{ij} - \zeta^i \zeta^j$. This is the root cause of Hall coefficient without a magnetic field. The intuitive understanding of the anomalous Hall response $\sigma^{xy} \sim \zeta^1 \zeta^2$ come from the small tilt limit where the tilt can be viewed as a boost parameter that converts the electric field into a magnetic field, whereby a Hall response can be generated. But our theory is not limited to small tilts and is valid for arbitrary tilts.

The second non-trivial consequence of the structure of spacetime in these solids is appearance of an additional contribution to the heat current that depends on the duration of the exposure to driving electrochemical potential gradients or thermal gradients. We dub *accumulative currents* to describe these type of heat current.

The third non-trivial and perhaps the most important aspect of transport in tilted Dirac materials which might have far reaching technological consequences is that a temporal gradient of temperature or electrochemical potential can be converted into electric or heat currents. The fact that

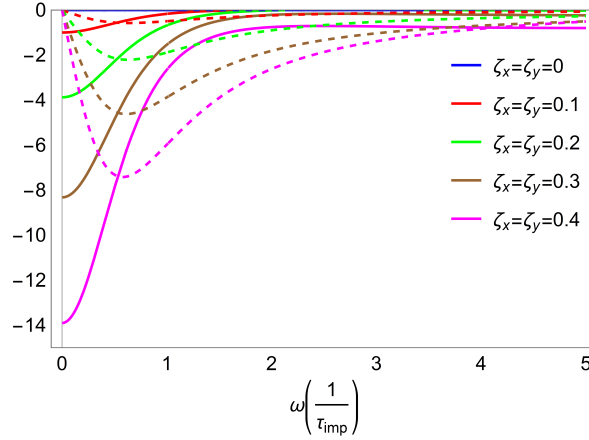


Figure 8: Real part (solid-line) and imaginary part (dashed-lines) of σ^{xy} for viscous fluid of TDFs at $T=150$ K in units of $[\frac{1}{mev \cdot \tau_{imp}}]$.

the nature provides free $\partial_t T$ in hot deserts from mid-night to mid-day might transform this unique capability of TDFs into a technological concept. This property arises, because the structure of spacetime in tilted Dirac fermion solids is such that it allows for a mixing between space and time coordinates. The intuitive explanation of this effect is as follows: When the system is heated, i.e. $\partial_t T > 0$, in the absence of tilt, the entire heat goes into random motion of electron. A system with a non-zero tilt is related to the one with zero tilt by a Galilean boost. Boosting a random kinetic motion of electrons will give rise to a net current. Therefore it is not surprising that temporal gradients can drive currents, pretty much the same way spatial gradients can drive currents. We have introduced the notion of *vector* transport coefficients (as opposed to commonly used, *tensor* ones), to formalize and quantify these effects. The important technological advantage of such effects is that, via the vector transport coefficient β^i , a gradual heating of these materials ($\partial_t T$) generates electric currents. Furthermore we find that this transport coefficient is given by $\beta^i = \sigma_Q \zeta^i$ which is nothing but the ability σ_Q of the material to conduct and the tilt vector ζ .

Typical industrial heating rates are on the scale of $\partial_t T \sim 0.4 \times 10^3$ K/s [58]. When combined with a typical Fermi velocity $v_F \sim 10^6$ m/s will be equivalent to a spatial gradient of $\partial_x T = v_F^{-1} \partial_t T \sim 0.4 \times$ K/mm. This is comparable to a typical temperature gradients in thermoelectric devices⁴. Therefore the vector transport coefficients are easily observable effects in the laboratory. As for the natural sources of the $\partial_t T$ in the desert, a typical temperature span of 40K during half cycle of earth rotation $\sim 40 \times 10^3$ s will give 10^{-3} K/s which is nearly 5 orders of magnitude smaller than the above value achievable in the laboratory.

Our theory presented in this paper is for a single Dirac cone. When it comes to realistic materials, one challenge of using this source of electricity is that since the transport coefficient β^i is proportional to ζ^i , in those materials where the number of Dirac nodes is even and are time reversal symmetric, such that for every tilted Dirac cone, there is another tilted Dirac cone with opposite ζ^i , these transport coefficients cancel each other's effect. In tilted Weyl materials that break the time reversal symmetry, the two nodes do have arbitrary tilt vector ζ , and the above effect survives. However, in time reversal symmetric Dirac/Weyl materials the effect of two tilted nodes cancel each other in the bulk. To remedy this, either one has to search for tilted Dirac cone materials with odd number of Dirac cones [53], or

⁴Larger values of the spatial gradients give rise to nonlinear effects. We thank Prof. K. Esfarjani for this discussion.

if they have even number of Dirac nodes, one has to search in lattices with broken time reversal symmetry that violates $\zeta_+ = -\zeta_-$. This can be extrinsically done by combining the sheets of Dirac materials with a magnetic layer.

Even if none of these systems are available still certain boundaries tend to prevent the cancellation: Building on the ideas of valleytronics [55, 56], populating a system of TDFs that possesses even number of Dirac nodes with $\zeta_+ = -\zeta_-$, appropriately chosen *boundaries* in nano-electronic devices can still give rise to out-of-equilibrium valley polarization effects that will eventually generate a non-zero total current from temporal gradients of \vec{T} (and/or μ). In fact in such valleytronics setup, the valley polarization translates into an effective ζ polarization which therefore activates a net non-zero vector transport coefficient. The corresponding heat transport coefficient γ^i makes materials with TDFs a suitable candidate in applications that require to direct the heat current into a given direction. This direction in TDFs is set by ζ . Such a preferred direction is reminiscent of non-reciprocal spin currents in gradient materials [59].

The heating of a TDF material (corresponding to $\partial_t T > 0$) converts the heat to the work. This corresponds to the charging stage if this effect is used to construct a battery. The reverse situation, namely cooling with $\partial_t T < 0$ corresponds to the discharge stage of the battery where battery does work on the environment during which the heat is extracted from the system.

Acknowledgements

S. A. J. thanks M. Mohajerani for providing an inspiring working environment during the COVID-19 outbreak. M. T. is supported by the research deputy of Sharif University of Technology. We appreciate helpful comments from the following colleagues: Reza Mansouri, Sohrab Rahvar, Sadamichi Maekawa, Farhad Shahbazi, Nima Khosrawi, Shant Baghran, Mehdi Kargarian, Abolhassan Vaezi, Saeed Abedinpour, Ali Esfandiari, Reza Ejtehadi, Takami Tohyama and Keivan Esfarjani.

Funding information This project was supported by the Iran Science Elites Federation (ISEF) and the deputy of research, Sharif University of Technology, grant No. G960214.

References

- [1] R. K. Pathria and P. D. Beale, *Statistical Mechanics*, Wiley Online Library (2007).
- [2] S. M. Girvin and K. Yang, *Modern Condensed Matter Physics*, Cambridge University Press, New York (2019).
- [3] M. S. Dresselhaus, *Group Theory: Applications to the Physics of Condensed Matter*, Springer (2008).
- [4] M. I. Katsnelson, *Graphene: Carbon in Two Dimension*, Cambridge University Press (2012).
- [5] X.-F. Zhou, X. Dong, A. R. Oganov, Q. Zhu, Y. Tian and H.-T. Wang, *Semimetallic two-dimensional boron allotrope with massless dirac fermions*, Phys. Rev. Lett. **112**, 085502 (2014), doi:10.1103/PhysRevLett.112.085502.
- [6] A. Lopez-Bezanilla and P. B. Littlewood, *Electronic properties of 8-*Pmmn* borophene*, Phys. Rev. B **93**, 241405 (2016), doi:10.1103/PhysRevB.93.241405.

- [7] N. Tajima, S. Sugawara, M. Tamura, Y. Nishio and K. Kajita, *Electronic phases in an organic conductor α -(BEDT-TTF) $_2$ I $_3$: Ultra narrow gap semiconductor, superconductor, metal, and charge-ordered insulator*, Journal of the Physical Society of Japan **75**(5), 051010 (2006).
- [8] S. Katayama, A. Kobayashi and Y. Suzumura, *Pressure-induced zero-gap semiconducting state in organic conductor α -(BEDT-TTF) $_2$ I $_3$ salt*, Journal of the Physical Society of Japan **75**(5), 054705 (2006), doi:10.1143/jpsj.75.054705.
- [9] A. Kobayashi, S. Katayama, Y. Suzumura and H. Fukuyama, *Massless fermions in organic conductor*, Journal of the Physical Society of Japan **76**(3), 034711 (2007), doi:10.1143/jpsj.76.034711.
- [10] A. Kobayashi, S. Katayama and Y. Suzumura, *Theoretical study of the zero-gap organic conductor α -(BEDT-TTF) $_2$ I $_3$* , Science and Technology of Advanced Materials **10**(2), 024309 (2009), doi:10.1088/1468-6996/10/2/024309.
- [11] N. Tajima and K. Kajita, *Experimental study of organic zero-gap conductor α -(BEDT-TTF) $_2$ I $_3$* , Science and Technology of Advanced Materials **10**(2), 024308 (2009), doi:10.1088/1468-6996/10/2/024308.
- [12] H. Isobe, *Tilted dirac cones in two dimensions*, In *Theoretical Study on Correlation Effects in Topological Matter*, pp. 63–81. Springer Singapore, doi:10.1007/978-981-10-3743-6_3 (2017).
- [13] M. O. Goerbig, J.-N. Fuchs, G. Montambaux and F. Piéchon, *Tilted anisotropic dirac cones in quinoid-type graphene and α -(BEDT-TTF) $_2$ I $_3$* , Phys. Rev. B **78**, 045415 (2008), doi:10.1103/PhysRevB.78.045415.
- [14] M. O. Goerbig, J.-N. Fuchs, G. Montambaux and F. Piéchon, *Electric-field-induced lifting of the valley degeneracy in α -(bedt-ttf) $_2$ I $_3$ dirac-like landau levels* **85**(5), 57005 (2009), doi:10.1209/0295-5075/85/57005.
- [15] S. A. Jafari, *Electric field assisted amplification of magnetic fields in tilted dirac cone systems*, Physical Review B **100**(4) (2019), doi:10.1103/physrevb.100.045144.
- [16] L. Liang and T. Ojanen, *Curved spacetime theory of inhomogeneous weyl materials*, Phys. Rev. Res. **1**, 032006 (2019), doi:10.1103/PhysRevResearch.1.032006.
- [17] A. Westström and T. Ojanen, *Designer curved-space geometry for relativistic fermions in weyl metamaterials*, Phys. Rev. X **7**, 041026 (2017), doi:10.1103/PhysRevX.7.041026.
- [18] G. E. Volovik, *Black hole and hawking radiation by type-II weyl fermions*, JETP Letters **104**(9), 645 (2016), doi:10.1134/s0021364016210050.
- [19] T. Farajollahpour, Z. Faraei and S. A. Jafari, *Solid-state platform for space-time engineering: The S_{pmn} borophene sheet*, Phys. Rev. B **99**, 235150 (2019), doi:10.1103/PhysRevB.99.235150.
- [20] Y. Yekta, H. Handipour and S. A. Jafari, *The formation and control of tilt in the dirac cone by atomic scale manipulation*, In preparation (2021).
- [21] A. Motavassal and S. A. Jafari, *Circuit realization of tilted dirac cone: A platform for fabrication of curved spacetime geometry on a chip* (2021), arXiv:2110.01906.

- [22] Z. Faraei and S. A. Jafari, *Perpendicular andreev reflection: Solid-state signature of black-hole horizon*, Phys. Rev. B **100**, 245436 (2019), doi:10.1103/PhysRevB.100.245436.
- [23] Z. Faraei and S. Jafari, *Electrically charged andreev modes in two-dimensional tilted dirac cone systems*, arXiv preprint arXiv:1912.06355 (2019).
- [24] Y. Kedem, E. J. Bergholtz and F. Wilczek, *Black and white holes at material junctions*, arXiv preprint arXiv:2001.02625 (2020).
- [25] I. Carusotto, S. Fagnocchi, A. Recati, R. Balbinot and A. Fabbri, *Numerical observation of hawking radiation from acoustic black holes in atomic bose–einstein condensates*, New Journal of Physics **10**(10), 103001 (2008), doi:10.1088/1367-2630/10/10/103001.
- [26] D. Gerace and I. Carusotto, *Analog hawking radiation from an acoustic black hole in a flowing polariton superfluid*, Physical Review B **86**(14) (2012), doi:10.1103/physrevb.86.144505.
- [27] H. Nguyen, D. Gerace, I. Carusotto, D. Sanvitto, E. Galopin, A. Lemaître, I. Sagnes, J. Bloch and A. Amo, *Acoustic black hole in a stationary hydrodynamic flow of microcavity polaritons*, Physical Review Letters **114**(3) (2015), doi:10.1103/physrevlett.114.036402.
- [28] A. Roldán-Molina, A. S. Nunez and R. Duine, *Magnonic black holes*, Physical Review Letters **118**(6) (2017), doi:10.1103/physrevlett.118.061301.
- [29] T. C. Wu, H. K. Pal, P. Hosur and M. S. Foster, *Power-law temperature dependence of the penetration depth in a topological superconductor due to surface states*, Phys. Rev. Lett. **124**, 067001 (2020).
- [30] R. N. Gurzhi, *HYDRODYNAMIC EFFECTS IN SOLIDS AT LOW TEMPERATURE*, Soviet Physics Uspekhi **11**(2), 255 (1968), doi:10.1070/pu1968v011n02abeh003815.
- [31] D. A. Teaney, *Viscous hydrodynamics and the quark gluon plasma*, In R. C. Hwa and X.-N. Wang, eds., *Quark-gluon plasma 4*, pp. 207–266, doi:10.1142/9789814293297_0004 (2010).
- [32] T. Schaefer and D. Teaney, *Nearly Perfect Fluidity: From Cold Atomic Gases to Hot Quark Gluon Plasmas*, Rept. Prog. Phys. **72**, 126001 (2009), doi:10.1088/0034-4885/72/12/126001.
- [33] K. Jensen, M. Kaminski, P. Kovtun, R. Meyer, A. Ritz and A. Yarom, *Parity-Violating Hydrodynamics in 2+1 Dimensions*, JHEP **05**, 102 (2012), doi:10.1007/JHEP05(2012)102.
- [34] D. T. Son and P. Surowka, *Hydrodynamics with Triangle Anomalies*, Phys. Rev. Lett. **103**, 191601 (2009), doi:10.1103/PhysRevLett.103.191601.
- [35] J. Bhattacharya, S. Bhattacharyya, S. Minwalla and A. Yarom, *A Theory of first order dissipative superfluid dynamics*, JHEP **05**, 147 (2014), doi:10.1007/JHEP05(2014)147.
- [36] P. Kovtun, D. T. Son and A. O. Starinets, *Viscosity in strongly interacting quantum field theories from black hole physics*, Phys. Rev. Lett. **94**, 111601 (2005), doi:10.1103/PhysRevLett.94.111601.
- [37] A. Buchel, *On universality of stress-energy tensor correlation functions in supergravity*, Phys. Lett. **B609**, 392 (2005), doi:10.1016/j.physletb.2005.01.052.

- [38] V. E. Hubeny, S. Minwalla and M. Rangamani, *The fluid/gravity correspondence*, In *Black holes in higher dimensions*, pp. 348–383, [817(2011)] (2012).
- [39] G. Policastro, D. T. Son and A. O. Starinets, *From AdS / CFT correspondence to hydrodynamics*, JHEP **09**, 043 (2002), doi:10.1088/1126-6708/2002/09/043.
- [40] S. Sachdev, *Quantum phase transitions*, Wiley Online Library (2007).
- [41] A. Lucas and K. C. Fong, *Hydrodynamics of electrons in graphene*, Journal of Physics: Condensed Matter **30**(5), 053001 (2018), doi:10.1088/1361-648x/aaa274.
- [42] M. Müller, J. Schmalian and L. Fritz, *Graphene: A nearly perfect fluid*, Phys. Rev. Lett. **103**, 025301 (2009), doi:10.1103/PhysRevLett.103.025301.
- [43] R. Bistritzer and A. H. MacDonald, *Hydrodynamic theory of transport in doped graphene*, Phys. Rev. B **80**, 085109 (2009), doi:10.1103/PhysRevB.80.085109.
- [44] L. Levitov and G. Falkovich, *Electron viscosity, current vortices and negative nonlocal resistance in graphene*, Nature Physics **12**(7), 672 (2016), doi:10.1038/nphys3667.
- [45] D. A. Bandurin, A. V. Shytov, L. S. Levitov, R. K. Kumar, A. I. Berdyugin, M. B. Shalom, I. V. Grigorieva, A. K. Geim and G. Falkovich, *Fluidity onset in graphene*, Nature Communications **9**(1) (2018), doi:10.1038/s41467-018-07004-4.
- [46] P. Kovtun, *Lectures on hydrodynamic fluctuations in relativistic theories*, Journal of Physics A: Mathematical and Theoretical **45**(47), 473001 (2012), doi:10.1088/1751-8113/45/47/473001.
- [47] C. Eckart, *The thermodynamics of irreversible processes. iii. relativistic theory of the simple fluid*, Physical review **58**(10), 919 (1940).
- [48] L. D. Landau and E. M. Lifshitz, *Fluid mechanics* (1959).
- [49] S. M. Carroll, *Spacetime and geometry*, Cambridge University Press (2019).
- [50] S. Weinberg, *Gravitation and cosmology: principles and applications of the general theory of relativity* (1972).
- [51] Z. Jalali-Mola and S. A. Jafari, *Electrodynamics of tilted dirac and weyl materials: A unique platform for unusual surface plasmon polaritons*, Phys. Rev. B **100**, 205413 (2019), doi:10.1103/PhysRevB.100.205413.
- [52] P. Sengupta, Y. Tan, E. Bellotti and J. Shi, *Anomalous heat flow in 8-pmmn borophene with tilted dirac cones*, Journal of Physics: Condensed Matter **30**(43), 435701 (2018).
- [53] B.-J. Yang and N. Nagaosa, *Classification of stable three-dimensional dirac semimetals with nontrivial topology*, Nature Communications **5**, 4898 EP (2014), Article.
- [54] G. Grignani and G. W. Semenoff, *Introduction to some common topics in gauge theory of spin systems*, In G. Morandi, P. Sodano, A. Taglicozzo and V. Tognetti, eds., *Field Theories for Low-Dimensional Condensed Matter Systems: Spin Systems and Strongly Correlated Electrons*, chap. 6. Springer Verlag, Berlin Heidelberg (2000).

- [55] J. R. Schaibley, H. Yu, G. Clark, P. Rivera, J. S. Ross, K. L. Seyler, W. Yao and X. Xu, *Valleytronics in 2d materials*, Nature Reviews Materials **1**(11) (2016), doi:10.1038/natrevmats.2016.55.
- [56] A. Rycerz, J. Tworzydło and C. W. J. Beenakker, *Valley filter and valley valve in graphene*, Nature Physics **3**(3), 172 (2007), doi:10.1038/nphys547.
- [57] C.-K. Chiu, Y.-H. Chan, X. Li, Y. Nohara and A. P. Schnyder, *Type-ii dirac surface states in topological crystalline insulators*, Phys. Rev. B **95**, 035151 (2017).
- [58] H. Xu, X. Tong, X. Zhao, Y. Zhang and J. Peklenik, *Investigations on high heating rate and precision calibration of the thermoelectric characteristics of the tool and work materials*, CIRP Annals **32**(1), 47 (1983).
- [59] G. Okano, M. Matsuo, Y. Ohnuma, S. Maekawa and Y. Nozaki, *Nonreciprocal spin current generation in surface-oxidized copper films*, Phys. Rev. Lett. **122**, 217701 (2019).